Mon. Not. R. Astron. Soc. **336,** 611–620 (2002)

The measurement of rotational broadening in post-common-envelope binaries

James N. Bleach,[1,2]★ Janet H. Wood,[2,3] B. Smalley[2] and M. S. Catalán[2]

[1] *Kyoto University, Yukawa Institute for Theoretical Physics, Kitashirakawa, Sakyo-ku, Kyoto 606-8502, Japan*
[2] *Keele University, School of Chemistry and Physics, Keele, Staffordshire ST5 5BG*
[3] *San Diego State University, Department of Astronomy, San Diego, CA 92182-1221, USA*

Accepted 2002 June 18. Received 2002 April 8; in original form 2001 January 23

ABSTRACT

We employ high-resolution echelle spectroscopy to measure the projected rotational velocity, $V_{\rm rot} \sin i$, in the post-common-envelope binaries EG UMa, HZ 9 and RE J1629 + 780. For EG UMa we obtain consistent $V_{\rm rot} \sin i$ measurements from the Na I doublet at 8183, 8195 Å (31.2 ± 3.7 km s^{-1}), the Fe and Ti intrinsically narrow metal (INM) lines in the region 8374–8430 Å (26.6 ± 2.7 and 27.8 ± 3.0 km s^{-1}) and the K I line at 7698.9 Å (26.2 ± 3.5 km s^{-1}). This is in contrast to previous measurements of $V_{\rm rot} \sin i$ from the Na I doublet and INM features derived using lower-resolution spectra, which were not consistent. Possible origins for the disagreement observed previously are discussed, including the inaccurate removal of telluric absorption. The values of $V_{\rm rot} \sin i$ measured from the high-resolution EG UMa spectra are also consistent with that expected from system parameters derived from previous observational data. We also update the ephemeris and orbital period of EG UMa.

We obtained rotation rate measurements of 34.3 ± 3.8 km s^{-1} for HZ 9 and 25.1 ± 2.3 km s^{-1} for RE J1629 + 780, as measured from the Na I doublet at 8183, 8195 Å and the INM lines. In both systems there is agreement between the $V_{\rm rot} \sin i$ values measured from the two regions. The value of $V_{\rm rot} \sin i$ measured in HZ 9 is similar to that measured for EG UMa. This is expected, as these systems share a similar orbital period and secondary star spectral type. The measurement of $V_{\rm rot} \sin i$ in RE J1629 + 780 indicates that this system, which lacks radial velocity shifts due to orbital motion, is a wide binary as opposed to a low-inclination system.

Key words: binaries: close – stars: individual: EG UMa – stars: individual: HZ 9 – stars: individual: RE J1629 + 780 – stars: rotation.

1 INTRODUCTION

Post-common-envelope binaries (PCEBs) are close, detached binary systems that consist of a white dwarf, or white dwarf precursor, primary star and a late-type, low-mass, main-sequence secondary star. They are thought to have originated from wider binaries that lost the majority of their angular momentum as a result of evolution through a common-envelope phase (Paczyński 1976; Iben & Livio 1993; Iben & Tutukov 1993; Sandquist et al. 1998). Here the more massive star evolves into its giant phase whilst the less massive component is still within its main-sequence lifetime. Mass transfer occurs on to the main-sequence star at a rate faster than that at which the star can accrete whilst maintaining hydrostatic equilibrium; the main-sequence star then also fills its Roche lobe and the entire system is engulfed by a common envelope. Interaction between common-envelope material and the stellar cores results in dissipation of the orbital energy; consequently the two cores spiral together and decrease their orbital separation. The interaction process produces enough thermal pressure to drive the ejection of the common envelope from the system. This is seen as an expanding planetary nebula, leaving behind the remnant, close, detached binary consisting of a subdwarf or white dwarf star in orbit with a low-mass, main-sequence star. In this paper we present echelle spectroscopy of three PCEBs: EG UMa, HZ 9 and RE J1629 + 780.

1.1 EG UMa

The white dwarf in EG UMa was discovered by Stephenson (1960), and Greenstein (1965) noted the presence of emission lines in the EG UMa spectrum indicating the existence of an unresolved companion. From the radial velocity variation of the Hα emission line, emanating from this M dwarf component alone, Lanning (1982) measured the orbital period to be ∼16 h.

Using model atmosphere analysis of the UV energy distribution and Lyα red wing, Sion, Wesemael & Guinan (1984) found that

★E-mail: jamesb@yukawa.kyoto-u.ac.jp

the white dwarf in EG UMa is considerably cooler than the white dwarfs found in similar systems, with a temperature of 13000 ± 500 K. Catalán, Welsh & Wood (2002b) are in agreement, after obtaining a temperature of 13125 ± 125 K from simultaneous wide-wavelength-coverage optical spectrum fits with a white dwarf spectrum and red dwarf spectrum. This temperature indicated that the secondary star should not be significantly irradiated. The secondary star emission was subsequently confirmed as arising from intrinsic chromospheric activity by Bleach et al. (2000). The low white dwarf temperature also results in EG UMa being a particularly good system in which to make secondary star $V_{\rm rot} \sin i$ measurements, as the red dwarf flux strongly dominates the observed flux in the far red (based on the fits of Catalán et al. 2002b). The secondary star in EG UMa has been classified as an M4V by measuring the TiO band ratios (Catalán et al. 2002b), which is in agreement with previous classifications of M4V from its derived magnitude (Sion et al. 1984) and M4.5V by *JHK* photometry (Probst 1984).

The $V_{\rm rot} \sin i$ of the secondary star in EG UMa was measured, from the Na I 8183, 8195 Å doublet, to be 54.5 ± 5 km s^{-1} (Bleach et al. 2000). The nearby Fe and Ti intrinsically narrow metal (INM) lines were found to give consistently lower values of $V_{\rm rot} \sin i$ compared to this Na I doublet measurement. In addition, the values of $V_{\rm rot} \sin i$ measured were inconsistent with other measured parameters and were deemed too unreliable to be the basis for full system parameter calculations. A complete set of system parameters for EG UMa were derived, however, based upon the measurement of K_2 and previous observational data (see table 5 of Bleach et al. 2000). The McDonald Observatory spectroscopy presented in Bleach et al. (2000) will be referred to on occasions throughout this work, and so we will define it here as simply the McDonald data.

1.2 HZ 9

HZ 9 was discovered by Humason & Zwicky (1947) in their search for faint blue stars. Owing to the presence of emission lines it was suggested that HZ 9 was an unresolved binary composed of a white dwarf and a dMe star (Greenstein 1958; Eggen & Greinstein 1965), and this was subsequently confirmed (Pesch 1968). Lanning & Pesch (1981) measured the period of this spectroscopic binary to be ∼13.5 h, with the system components identified as a DA white dwarf and a main-sequence dM4.5e star. Guinan & Sion (1984) used *IUE* spectroscopy of the degenerate component to obtain an effective temperature and gravity of 20 000 ± 2000 K, $\log g = 8 \pm 0.2$ for the DA2 primary star. Catalán et al. (2002b) are in good agreement, obtaining values of 20 166 ± 623 K, $\log g = 7.81 \pm 0.24$ and 17 750 ± 1500 K, $\log g = 8.25 \pm 0.30$ from Balmer line and wide-wavelength-coverage optical spectrum fits, respectively. Catalán et al. (2002b) also used TiO band measurements to estimate a spectral type of M4V for the secondary star.

1.3 RE J1629 + 780

RE J1629 + 780 was first discovered by the *ROSAT* Wide Field Camera (WFC) as a bright source of extreme ultraviolet (EUV) radiation, and was included in the subsequent WFC all-sky survey (Pounds et al. 1993). Cooke et al. (1992) identified that RE J1629 + 780 was a binary system consisting of a hot DA white dwarf primary star and an M dwarf secondary star, most probably of spectral type dM2 to dM5. Sion et al. (1995) analysed optical and far-ultraviolet spectroscopy and obtained a temperature of 42 500 ± 1300 K, $\log g = 7.6 \pm 0.3$ for the DA2 white dwarf. The optical data revealed variable emission-line strength but no evidence of wavelength shifts reflecting orbital motion, interpreted as suggesting that the two component stars of the binary are widely separated.

Catalán et al. (1995) used the TiO band ratio from low-resolution spectroscopy (3400–8900 Å) to estimate the spectral type of the secondary star to be dM4. They used hydrogen model fits to Balmer absorption features to derive a temperature of 41 800 ± 2000 K and $\log g = 8.0 \pm 0.5$ for the white dwarf, in good agreement with that obtained by Sion et al. (1995). An alternative configuration for the binary system was discussed by Catalán et al. (1995) in which RE J1629+780 is a very low-inclination system and does not necessarily have to be a long-period binary.

1.4 Rotational broadening

The method of projected rotational velocity, $V_{\rm rot} \sin i$, measurement employed in this work involves fitting broadened template spectra to a target spectrum, varying the broadening applied to the templates to identify the best value for the rotational broadening in the target (for more details on $V_{\rm rot} \sin i$ measurement, see Section 3.2). This technique is in common use in cataclysmic variables (CVs) (e.g. Horne, Welsh & Wade 1993; Shahbaz & Wood 1996), low-mass X-ray binaries (LMXBs) (e.g. Marsh, Robinson & Wood 1994; Casares & Charles 1994) and post-common-envelope binaries (PCEBs) (e.g. Bleach et al. 2000; Catalán et al. 2002b).

However, concerns about the accuracy of this technique do exist. $V_{\rm rot} \sin i$ measurements obtained from the 8183, 8195 Å Na I doublet have been found to be consistently higher than those measured from the nearby INM lines, both in the PCEBs EG UMa (Bleach et al. 2000) and PG 1026 + 002 (Catalán et al. 2002b) and in M dwarf stars (Catalán, Smith & Jones 2002a). These are the only previous studies to compare the value of $V_{\rm rot} \sin i$ measured from the 8183, 8195 Å Na I doublet to that measured from other photospheric lines. Furthermore, Na I doublet $V_{\rm rot} \sin i$ measurements in PCEBs have been found to be inconsistent with other measured system parameters (EG UMa and PG 1026 + 002, Bleach et al. 2000; PG 1026 + 002 and RE J2013 + 400, Catalán et al. 2002b). However, no firm conclusions could be drawn on the origin of the inconsistencies from these previous studies, which were derived from medium-resolution data. Echelle observations were thus obtained to explore the measurement of $V_{\rm rot} \sin i$ at high resolution.

This work investigates the measurement of $V_{\rm rot} \sin i$ from the Na I doublet at 8183, 8195 Å,[1] the INM lines (in the region 8374–8430 Å) and the K I line at 7698.9 Å. An investigation into the suitability of the Na I doublet photospheric feature for the measurement of $V_{\rm rot} \sin i$ is of particular importance as, in addition to proving problematic in the past, it can be the only strongly detectable, and measurable, secondary star feature in CV and LMXB systems [see Smith et al. (1997) for a survey of the Na I doublet in CVs]. Its detectability is due to strong linestrength combined with the fact that the contribution of the cool secondary star to total system flux increases towards this far-red wavelength region. This increased contribution is due to both the augmented red dwarf flux and the reduced white dwarf and accretion disc fluxes.

PCEBs offer an excellent environment in which to test the measurement of the projected rotational velocity, and to investigate which spectral lines should be employed, as no mass transfer is

[1] This is in fact a triplet with line centres at 8183.25, 8194.79 and 8194.82 Å. However, the latter 8194.8 Å doublet is unresolved.

occurring and geometric distortions are small. Secondary star features are often more easily detected and analysed as the system flux is not dominated by a bright accretion disc such as in CVs and other semidetached systems. One potential concern is that the secondary stars in PCEBs may exhibit abundance anomalies as a result of mass transfer during the common-envelope phase of evolution. This could render them unsuitable for $V_{\rm rot}\sin i$ measurement. However, an abundance analysis of the PCEB EG UMa (Rushton et al., in preparation) has ruled out, at least for this system, the presence of any anomalies in the spectral lines studied in this work.

In Section 2 we describe the observations taken and data reduction procedure followed. Section 3 presents the results and analysis of the EG UMa data, and Section 4 the results and analysis of the HZ 9 and RE J1629 + 780 data. A summary of the conclusions that we draw from this work is presented in Section 5.

2 OBSERVATIONS AND THEIR REDUCTION

2.1 Echelle spectroscopy

Observations were taken on the nights of 1998 March 18/19 and 19/20 at the 4.2-m William Herschel Telescope (WHT) using the Utrecht Echelle Spectrograph (UES) with the 2048 × 2048 pixel SITe1 charge-coupled device (CCD) as detector. The echelle 31 grating (31.6 groove mm^{-1}) was employed with a dispersion ranging from 0.04 to 0.09 Å pixel^{-1}. The central wavelength was 5430 Å, with a wavelength range from ∼4250 to 9000 Å covered in ∼74 orders. A summary of the target observations is given in Table 1.

Thorium–argon lamp exposures were taken for wavelength calibration and tungsten lamp exposures for flat-fielding. Spectra of the flux standards BD+75° 325, HZ 44 and Feige 66 were taken to fulfil roles in telluric absorption removal. A number of M dwarf spectra (see Table 2) were taken for use as rotational velocity templates.

The data were reduced using the Starlink ECHOMOP package (Mills, Webb & Clayton 1997). Calibration and spectral extraction were achieved using FIGARO (Shortridge et al. 1999). The blaze function in each order was removed from the spectra by normalizing with a polynomial fit to the observed continuum. An EG UMa spectral atlas covering the wavelength ranges 4325–4365 and 4845–8445 Å can be found in Bleach (2001).

3 EG UMa

3.1 Radial velocity of the secondary star

To update the EG UMa ephemeris, radial velocity measurements were obtained from the Rb I 7800.2 Å absorption line in each of the EG UMa spectra. The resulting radial velocity curve was considerably offset from the phase zero predicted using the ephemeris in Bleach et al. (2000). Radial velocity measurements were also obtained from the Ti I 8382.5 Å absorption line to rule out the possibility of the Rb I result being anomalous. A good agreement was immediately apparent between the measurements from these two absorption lines. The problem was found to lie with the initial choice of the offset of the blue to red crossing time of the radial velocity curve from the time of phase zero predicted using the ephemeris and period of Lanning (1982). Initially taken to be 0.102 73 (Bleach et al. 2000), it was just as possible that the offset was in fact −0.897 27; instead of being late by ∼0.1 of a phase, it was actually early by ∼0.9 of a phase. Thus it was an alias problem. Now that there exist three radial velocity curves for EG UMa, the offset of the WHT radial velocity curve from the time of phase zero predicted using the ephemeris and period of Lanning (1982) was −1.070 12 (cycle number 9902); an observed−calculated (O–C) fit was used to determine an updated ephemeris

$$\mathrm{HJD} = 244\,4279.9151(18) + 0.667\,578\,77(54).$$

The radial velocity curve produced using this ephemeris is shown in Fig. 1 and a sinusoidal fit results in a radial velocity semi-amplitude of 126.0 ± 2.5 km s^{-1}, in excellent agreement with previous measurements.

Table 1. Summary of WHT spectroscopic target observations.

Target	Exposure time(s)	Number of observations
EG UMa	600/1200/1431/1800	1/2/1/9[a]
HZ 9	1800	1
RE J1629 + 780	1800	1

[a]The nine 1800-s EG UMa exposures were labelled 1D–1G and 2A–2E due to the timing of their occurrence during the first and second night of observations respectively. This labelling is how EG UMa spectra will be referenced throughout this work.

Table 2. Information on the M dwarfs observed using WHT UES.

Name	Exposure time (s)	V mag.	Spectral type 1[a]	Spectral type 2[b]	$V_{\rm rot}\sin i$ (km s^{-1})[c]
Night 1					
Gl 486	480	11.8	M3.5V	M4.0V	<2.0
Gl 447	720	13.5	M4.0V	M4.5V	<2.0
Gl 548A	600	8.8	M0.0V	M1.0V	–
Gl 548B	600	9.1	M0.5V	M2.0V	–
Night 2					
Gl 403	1200	12.1	M3.5V	M3.0V	–
Gl 436	800	10.7	M2.5V	M3.5V	–
Gl 402	900	12.5	M4.0V	M5.0V	<2.3
Gl 406	1800	16.5	M5.5V	M6.0V	<2.9
Gl 699	600	13.2	M4.0V	M5.0V	<2.8

[a]Reid, Hawley & Gizis (1995).
[b]Gliese & Jahreiss (1991).
[c]$V_{\rm rot}\sin i$ measurements taken from Delfosse et al. (1998).

3.2 Rotational broadening

We obtained rotation rate, $V_{\rm rot}\sin i$, measurements for EG UMa from the Na I doublet at 8183, 8195 Å, single and groups of multiple INM lines (in the region 8374–8430 Å) and the K I line at 7698.9 Å. The method of $V_{\rm rot}\sin i$ measurement employed in this work, as outlined in Section 1.4, involves the application of a broadening function (Gray 1992) to a template star of the same spectral type as, or as close as is available to, the target. By choosing a suitable template star, we are assuming that the intrinsic linestrengths of the two stars are matched, and thus any difference in linewidths is due to a change in rotational velocity alone. The intrinsic rotational velocity of the late-type star templates has either been measured to be low (see Table 2) or is ignored under the assumption that the rotation rate has been reduced, via angular momentum loss processes, to be of the order of 1 km s^{-1} (Gray 1992).

The broadened template is then fitted to the data using an optimal subtraction routine, which, after the continuum is subtracted from

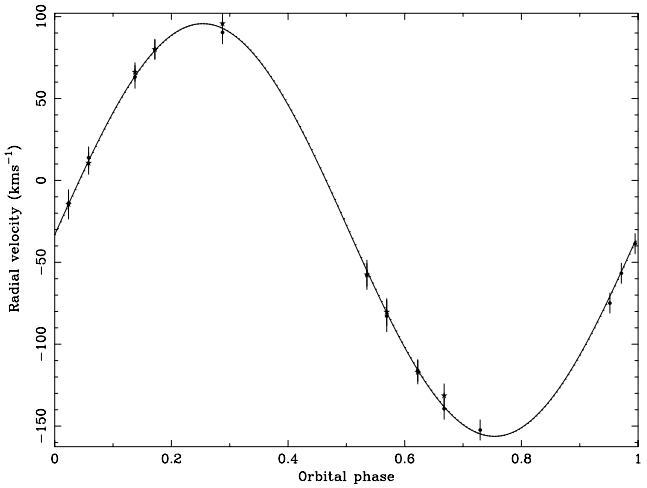

Figure 1. Radial velocity of the secondary star in EG UMa as measured from the Rb I 7800.2 Å line (points) and the Ti I 8382.5 Å line (stars). This radial velocity curve employs the ephemeris calculated using radial velocity offset information from the McDonald and echelle data with respect to the ephemeris of Lanning (1982) (see Section 3.1).

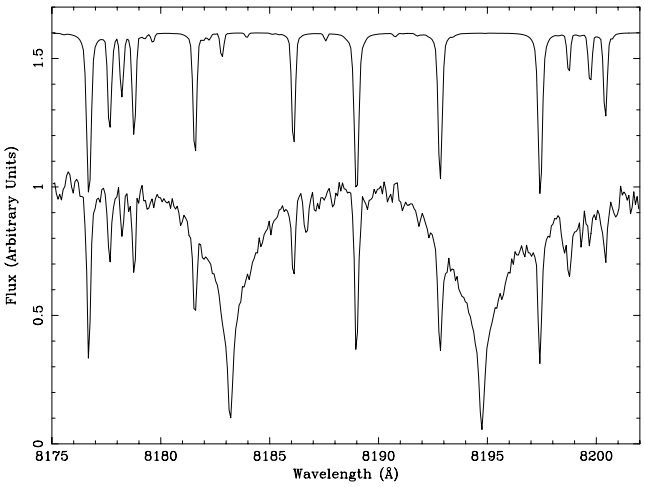

Figure 2. The Na I doublet of the M star Gl 402 (lower curve) and a synthetic telluric spectrum covering the same wavelength region (upper curve). All of the strong telluric lines can be identified within the observed spectrum. The synthetic spectrum has been vertically offset by +0.6 for clarity.

both object and template, subtracts constants times the template spectra from the object spectra, adjusting the constants to minimize the residual scatter between the spectra. The scatter is measured by carrying out the subtraction and then computing the χ^2 between this residual spectrum and a smoothed version of itself. The minimum of the distribution of χ^2 versus broadening values is then the best value for the rotational broadening.

3.2.1 Telluric absorption

The Na I doublet at 8183, 8195 Å, which is used to measure the rotational velocity of the secondary star, is positioned within a broad band of telluric absorption. A synthetic atmosphere spectrum was produced using the HITRAN 96 (Rothman et al. 1998) H_2O and O_2 line list and the Nicholls (1988) model of the Earth's atmosphere. Calculations were performed at the appropriate height above sea level and airmass for the observations. This synthetic atmosphere spectrum was used to identify the telluric lines present in the Na I doublet wavelength region (see Fig. 2). The high resolution of the echelle data facilitated the identification of all telluric lines within the observed spectra. This is extremely useful, as now each discrete telluric absorption line can be identified and masked or patched out of any analysis of the Na I doublet. Therefore, initially, no attempt was made to correct for the atmospheric water lines in the Na I spectra.

The problem with not removing the telluric lines is that the amount of data available for fitting is strongly curtailed. Telluric masking was applied to the wavelength regions 8176.35–8179.45, 8181.10–8182.50, 8185.74–8187.06, 8188.43–8190.17, 8192.32–8193.68 and 8196.96–8201.14 Å. Fig. 3 displays examples of the best and worst cases of water masking that occurred as a result of

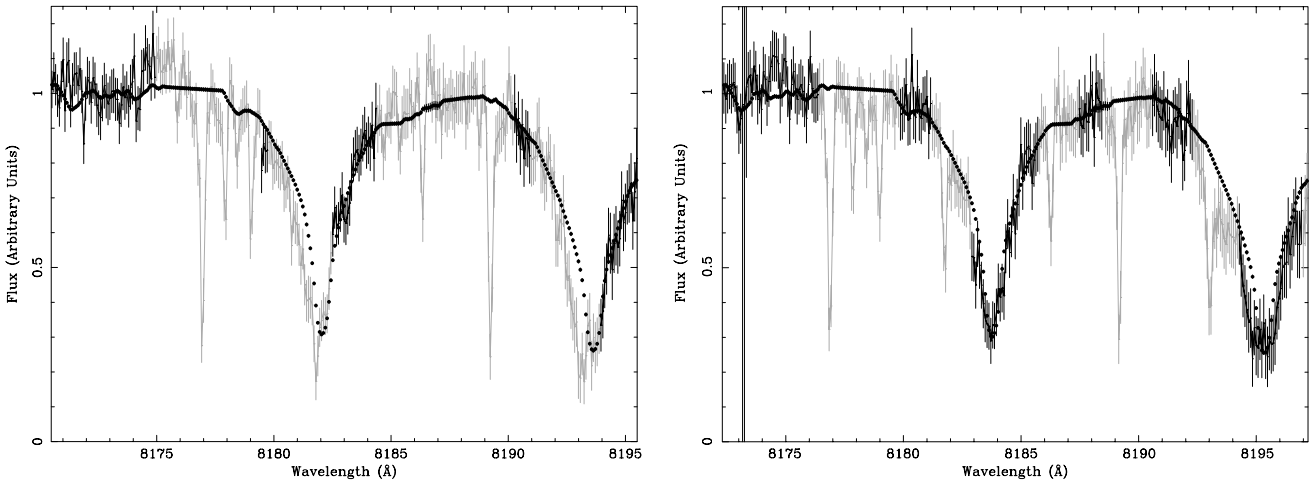

Figure 3. Left: Na I doublets of the EG UMa observation 2B (solid line) and the M star Gl 402 (points). Right: Na I doublets of the EG UMa observation 1E (solid line) and the M star Gl 402 (points). In each plot the Gl 402 Na I doublet has been scaled and shifted to fit the EG UMa observation. The wavelength regions affected by telluric absorption are shown in grey and do not contribute to the fit. The extent of this telluric masking is dependent on the radial velocity offset between the target and template spectra. In the worst scenario there is really very little of the line profile suitable for fitting (left-hand plot), and even in the best scenario significant amounts of data, and thus fitting information, are lost (right-hand plot).

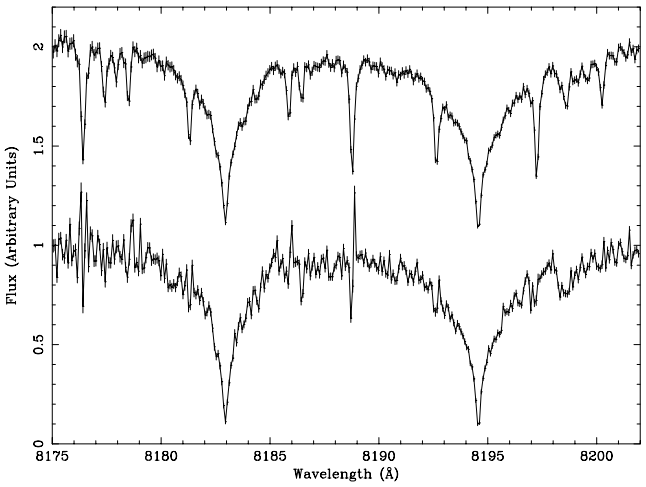

Figure 4. Na I doublets of the M star Gl 402 prior to (upper spectrum) and after (lower spectrum) correction for telluric absorption. The S/N has been reduced and some bad features remain in the corrected spectrum. The upper spectrum has been offset by +1 for clarity.

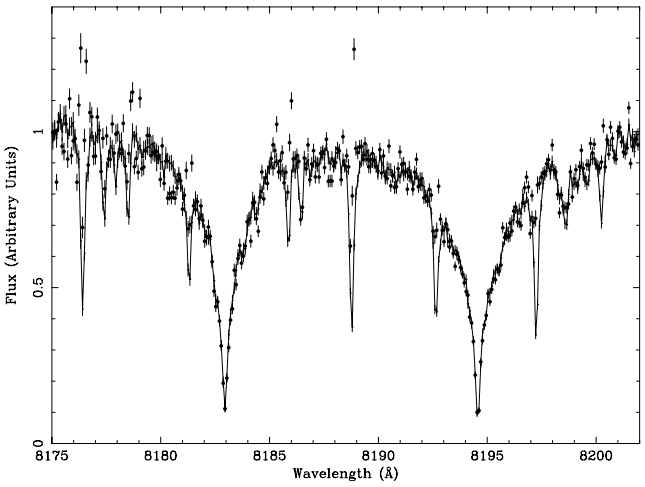

Figure 5. Na I doublets of the M star Gl 402 prior to (solid line) and after (points) correction for telluric absorption. The general doublet profile is well matched between the two spectra.

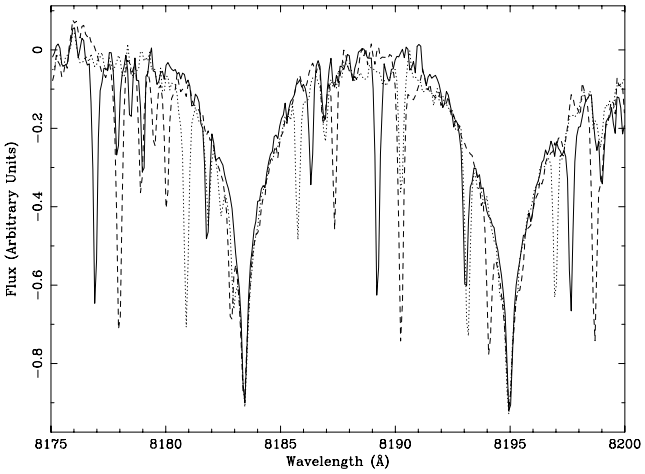

Figure 6. The Na I doublets of three M stars of comparable spectral type: dotted line, Gl 699(M4/5V); solid line, Gl 402 (M4/5V); broken line, Gl 447 (M4/4.5V). The majority of the other absorption lines displayed in this plot are telluric, being offset between each M star spectrum as a result of the correction for radial velocity.

differing radial velocity shifts between the object spectra (EG UMa observations 1E and 2B) and the template (Gl 447). Aligning the EG UMa and template star Na I doublets simultaneously offsets the telluric absorption lines, whose wavelength positions are unaffected by the stellar radial velocity. In the worst scenarios there is really very little of the line profile suitable for fitting, and even in the best scenarios significant amounts of data, and thus fitting information, are lost. A meaningful measurement of $V_{\rm rot}\sin i$ was not obtainable under such conditions.

The telluric absorption lines therefore had to be removed. This was attempted through multiplication by a telluric reference spectrum, or atmospheric template, created from a water standard star spectrum. Prior to multiplication, the template spectrum is scaled according to the ratio of the airmass between the object and the water template. The water lines were removed to varying degrees in different objects, but never completely satisfactorily (see Fig. 4). A further problem was the lack of a very high signal-to-noise ratio (S/N) standard star to be used as the water template; as a result there was a noticeable noise increase in the water-corrected spectra. A new attempt was made to remove the telluric lines, this time by scaling the synthetic telluric spectrum to match the observed lines. However, after attempted line removal, residual features remained, owing to the fact that the line profiles between the observed and synthetic spectra never exactly matched.

Telluric absorption is then a significant problem – it cannot be removed easily, and simply ignoring affected regions excludes large amounts of data. However, when telluric removal employing a telluric reference spectrum was applied, the general profiles of the Na I doublets were unaltered (see Fig. 5). To continue this investigation into $V_{\rm rot}\sin i$, we then had to remove the telluric absorption as best as possible and assume that fits to the Na I doublet profile were not significantly affected by any remnant bad pixels, and would thus provide us with an accurate measurement of $V_{\rm rot}\sin i$. Water correction was then undertaken via multiplication with a telluric reference spectrum.

3.2.2 Na I doublet analysis

Before any $V_{\rm rot}\sin i$ measurements were taken from the Na I doublet, we investigated whether the profile of this feature varied significantly between M stars of approximately matching spectral type. If variation did occur, this would indicate that any measurement of $V_{\rm rot}\sin i$ would be strongly dependent on the template star employed, and this feature would then be unsuitable for $V_{\rm rot}\sin i$ measurement. Fig. 6 shows that the Na I doublets from three M stars of close, and possibly exactly matched, spectral type display only a weak variation in Na I doublet profile. The value of $V_{\rm rot}\sin i$ measured using any of these three M stars should therefore be consistent, removing any template dependence. For comparison, Fig. 7 displays the Na I doublets from three M stars of differing spectral type. As expected, the strength of the Na I doublet increases with later spectral type (see for example Wade & Horne 1988).

We fitted two of the best S/N EG UMa Na I doublet observations (1E and 2C) employing two different template M stars (Gl 402 and GL 447), which were first smeared to incorporate the same radial velocity spread as occurs due to the binary motion in the respective EG UMa spectra. The wavelength range over which fitting of the

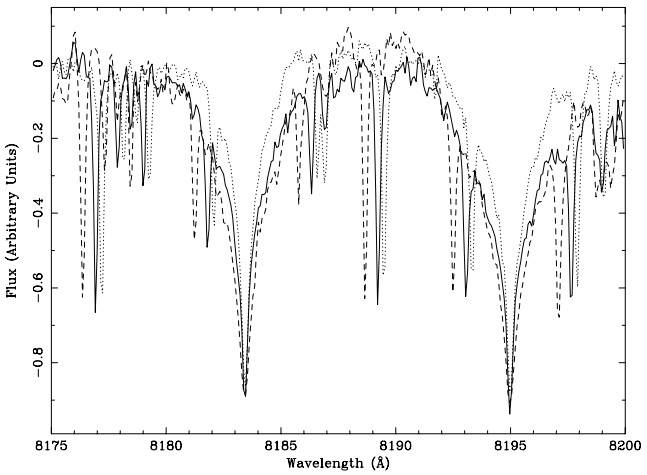

Figure 7. The Na I doublets of three M stars of differing spectral type: dotted line, Gl 548A (M0/1V); solid line, Gl 402 (M4/5V); broken line, Gl 406 (M5.5/6V). The majority of the other absorption lines displayed in this plot are telluric, being offset between each M star spectrum as a result of the correction for radial velocity.

Table 3. Summary of EG UMa $V_{\rm rot} \sin i$ measurements from observations 1E and 2C using the template stars Gl 447 (upper measurement) and Gl 402 (lower measurement).

Target line(s)	λ (Å)	$V_{\rm rot} \sin i$ (km s^{-1}) 1E	2C
Na I	8183.3, 8194.8	28.0 ± 7.0	32.0 ± 9.0
		31.0 ± 6.0	36.0 ± 9.0
Ti I	8382.5	27.0 ± 8.0	22.0 ± 15.0
		29.0 ± 7.0	25.0 ± 14.0
Fe I	8387.8	19.0 ± 8.0	27.0 ± 10.0
		20.0 ± 7.0	28.0 ± 10.0
Ti I	8426.5	24.0 ± 15.0	36.0 ± 9.0
		25.0 ± 12.0	36.0 ± 9.0

Na I doublet was employed was 8172–8197 Å; this range was chosen to avoid the region >8197 Å which contains V I, Zr I, Fe I and TiO lines (Schiavon et al. 1997). Rotational broadening was applied in steps of 1 km s^{-1} and the full range of the limb-darkening coefficient (0–1) was incorporated. The $V_{\rm rot} \sin i$ values measured from the Na I doublet are displayed in Table 3 and are all consistent with each other. A best fit to the EG UMa observation 2C employing the M star template Gl 402 is shown in Fig. 8. Fits were also carried out to EG UMa observation 1E using the template stars Gl 548A and GL 406. Values of 38 ± 8 km s^{-1} using Gl 548A and 26 ± 14 km s^{-1} with Gl 406 (with the larger error bar as a result of lower S/N) were obtained. The values of $V_{\rm rot} \sin i$ measured using template M stars of different spectral type are then all consistent with each other. This is probably a result of the variation of the Na I doublet with spectral type, shown in Fig. 7, being hidden within the noise of the EG UMa spectra.

3.2.3 *INM lines*

Measurements from the INM lines were again obtained from EG UMa observations 1E and 2C using the template stars Gl 402 and GL 447. The INM lines employed are not affected by telluric absorption. The $V_{\rm rot} \sin i$ values measured are displayed in Table 3 and are consistent with those measured from the Na I doublet. The best fit to the Ti I 8382.5 Å line is shown in Fig. 9. The disagreement between the values measured from the Na I doublet and the INM lines observed in the McDonald data is then not exhibited in the echelle data. Furthermore, these INM values are consistent with the majority of the single-line INM measurements from the McDonald data, indicating that they are the more trustworthy and suggesting the previous problem lies with the medium-resolution Na I doublet.

To try to reduce the error bar on the INM $V_{\rm rot} \sin i$ measurements, we fitted a number of INM lines simultaneously. On this occasion we fitted the EG UMa observation 2B, again chosen for its high S/N, with the M stars Gl 402, GL 447 and GL 699. The values of $V_{\rm rot} \sin i$ obtained (see Table 4) are all consistent. The origin of this agreement is clearly displayed in Fig. 10, which shows the excellent match between the INM line profiles of the three different M stars. What is more surprising is that these INM lines do not show any significant variation between spectral types [in contrast to the synthetic spectra of Allard and Hauschildt (see Allard & Hauschildt 1995; Hauschildt, Baron & Allard 1997, and references therein), which do exhibit some variation in INM line profiles over the temperature range of the M stars considered here]. $V_{\rm rot} \sin i$ measurements using the M stars Gl 548A and GL 436, whose spectral types do not match that of the secondary star in EG UMa, are in strong agreement with those measured from templates of matching spectral type (see Table 4). The remaining observed M stars, excluding Gl 406 whose S/N was too poor to allow a comparison of the INM lines, were also found to display very little variation in INM line profile across a range in M star spectral types (Gl 403, M3.5/3.0V; Gl 486, 3.5/4.0V; Gl 548B, 0.5/2.0V). This result has potentially very important connotations, because, if the $V_{\rm rot} \sin i$ values measured from these INM lines are correct, then this would completely remove any dependence on the spectral type of either the binary system M dwarf secondary star or the M star template. This could be extremely useful for the secondary stars in CV and LMXB systems where the spectral typing of the secondary star can be problematic, at least for systems in which the INM lines are detectable.

Finally, to measure a best possible single value of $V_{\rm rot} \sin i$ from the secondary star in EG UMa, we produced an average INM line spectrum from the nine 1800-s EG UMa observations. The spectra were aligned prior to averaging. Each individual EG UMa spectrum incorporated a different amount of smearing due to binary motion that contributed to the average EG UMa spectrum. To incorporate the same effect into the template spectrum, the template employed was in fact the average of nine spectra of the M star Gl 447. Each individual Gl 447 spectrum incorporated the amount of smearing present in one of the EG UMa spectra. The best fit was searched for in steps of 0.25 km s^{-1} and incorporated the full range of the limb-darkening coefficient (0–1). The value measured was 27.8 ± 3.0 km s^{-1}. This value is in excellent agreement with the value of 28.6 km s^{-1} predicted in Bleach et al. (2000), which was derived using the expected white dwarf mass and system mass ratio.

3.2.4 *K I 7698.9 Å line*

For comparison with the $V_{\rm rot} \sin i$ values measured from the Na I doublet and INM lines, we employed another secondary star photospheric spectral feature, the K I line at 7698.9 Å. Like the Na I doublet, the K I linestrength was found to increase with later spectral type. This line was chosen because of its strength; however, use of this line is restricted by the nearby location of very strong telluric

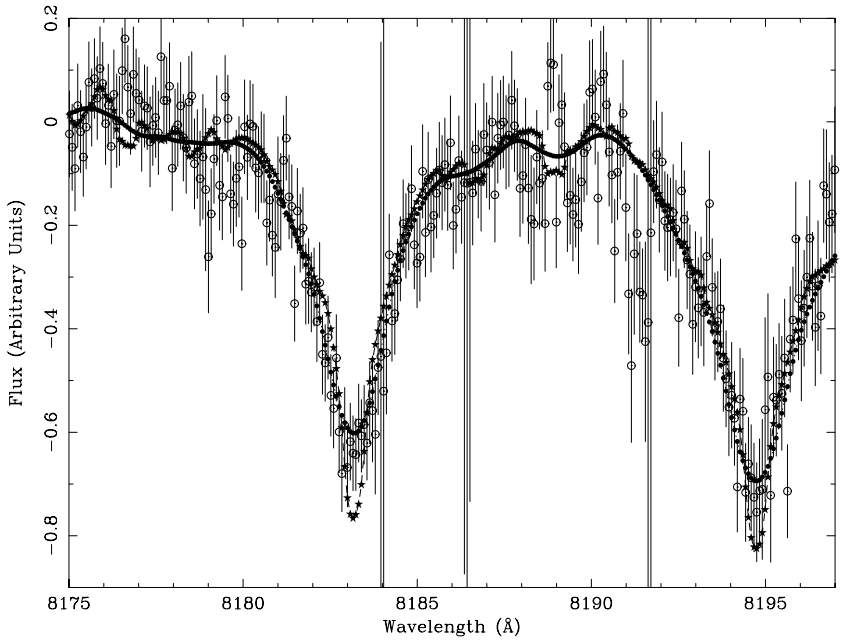

Figure 8. Broadened template fit (full circles) to the observed EG UMa Na I doublet (observation 2C, open circles). The best-fitting unbroadened template (stars) is also displayed for comparison. The broadened template was created from the M dwarf Gl 402 spectrum using $V_{\rm rot} \sin i = 38$ km s^{-1}, a limb-darkening coefficient of 1 and smearing to incorporate the EG UMa secondary star binary motion.

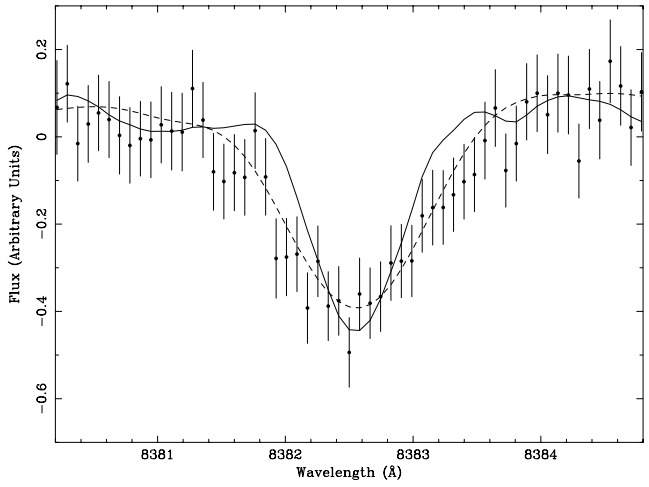

Figure 9. Broadened template fit (broken line) to the EG UMa 8382.5 Å Ti I line from observation 1E (points). The best-fitting unbroadened template (solid line) is also displayed for comparison. The broadened template was created from the M dwarf Gl 447 spectrum using $V_{\rm rot} \sin i = 25$ km s^{-1}, a limb-darkening coefficient of 0 and smearing to incorporate the EG UMa secondary star binary motion.

absorption. Telluric absorption also rules out the use of the blueward 7664.9 Å K I line. We chose to produce an average measured from the EG UMa observations 1D, 1E, 1F, 1G, 2A and 2B, as the radial velocities of these observations avoid water encroachment into the K I line profile. The fitting range employed was 7695–7703 Å, broadening was in steps of 0.25 km s^{-1} and zero to full limb darkening was incorporated. The $V_{\rm rot} \sin i$ values measured using the M stars Gl 447 and GL 402 were 26.0 ± 6.0 and 26.25 ± 4.25 km s^{-1} respectively. These values are then consistent with each other and with the measurements from the Na I doublet and INM lines. This

Table 4. Summary of INM multiline fit $V_{\rm rot} \sin i$ measurements from EG UMa observation 2B using a number of template stars. The fitting range employed covered 8374–8400 and 8410–8430 Å.

Template	$V_{\rm rot} \sin i$ (km s^{-1})
Gl 402	30.0 ± 4.0
Gl 447	31.0 ± 5.0
Gl 699	31.0 ± 5.0
Gl 436	30.0 ± 4.0
Gl 548A	30.0 ± 5.0

indicates a reassuring consistency in the value of $V_{\rm rot} \sin i$ measured from different secondary star photospheric lines.

3.2.5 $V_{\rm rot} \sin i$ *discussion*

To explore the possibility that the change in the value of $V_{\rm rot} \sin i$ measured from the Na I doublet, in the echelle data compared to the medium-resolution data, is a direct result of the change in the data resolution, we performed a number of tests with echelle spectra reduced to the resolution of the McDonald data set. To reduce the resolution of the echelle data, the spectra were smeared to incorporate the instrumental broadening, and then binned to the CCD pixel size of the McDonald data. The reduced-resolution echelle measurements obtained (see Table 5) are consistent with those measured at higher resolution (see Table 3), albeit with larger error bars. Therefore the change in resolution appears not, at least directly, to be the cause of the inconsistency between the McDonald and echelle Na I doublet measurements. This is in agreement with the tests undertaken on the McDonald data in Bleach et al. (2000), which concluded that the resolution of the McDonald data was good enough to obtain reliable $V_{\rm rot} \sin i$ measurements. Furthermore,

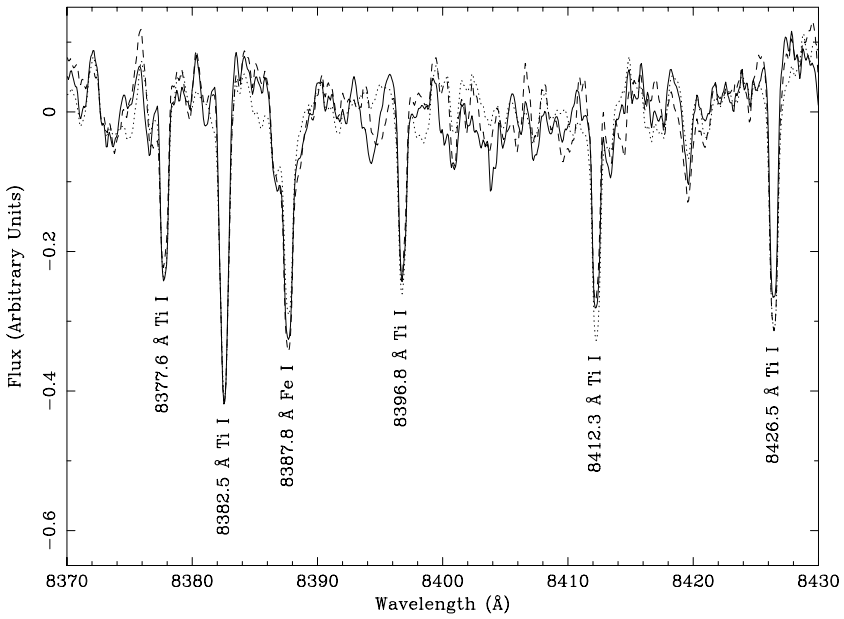

Figure 10. A selection of M star INM lines that have been smeared to incorporate the binary motion of the secondary star in EG UMa. These lines were fitted simultaneously to measure $V_{\rm rot} \sin i$. Solid line, Gl 402 (M4/5V); broken line, Gl 447 (M4/4.5V); dotted line, Gl 699(M4/5V).

Table 5. Summary of Na I doublet $V_{\rm rot} \sin i$ measurements obtained from different objects and using different templates, all at the resolution of the McDonald data set. Echelle data objects/templates degraded to the resolution of the McDonald data are followed by – degraded, original McDonald data objects/templates are followed by – McDonald.

Object	Template	$V_{\rm rot} \sin i$ (km s^{-1})
1E – degraded	Gl 402 – degraded	33.0 ± 13.0
1E – degraded	Gl 447 – degraded	41.0 ± 8.0
1E – degraded	Gl 699 – degraded	29.0 ± 10.0
1E – degraded	Gl 251 – McDonald	39.0 ± 11.0
EG UMa – McDonald	Gl 402 – degraded	48.0 ± 6.0
EG UMa – McDonald	Gl 447 – degraded	50.0 ± 5.0
EG UMa – McDonald	Gl 669A – McDonald	53.0 ± 5.5[a]

[a] Value taken from Bleach et al. (2000).

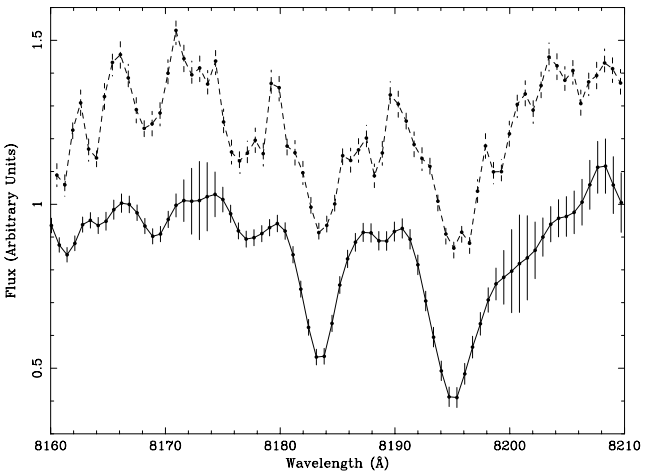

Figure 11. A typical McDonald EG UMa Na I doublet (upper spectrum) in comparison to a typical echelle EG UMa Na I doublet degraded to the resolution of the McDonald data (lower spectrum). Neither spectrum has been corrected for telluric absorption. The echelle observation clearly exhibits weaker telluric absorption than that present in the McDonald observation.

reduced-resolution echelle template stars and McDonald template stars can be interchanged whilst maintaining the consistency of the measured values (again see Table 5). This also rules out the M star templates as the origin of the discrepant measurements.

$V_{\rm rot} \sin i$ measurements were also taken from reduced-resolution INM lines, fitting over the same region as in Table 4. Once again the values obtained are in agreement with those measured at higher resolution (for example, 32 ± 12 km s^{-1} measured from observation 2B using the M star Gl 699). The inconsistency between the $V_{\rm rot} \sin i$ measurements from the Na I doublet and the INM lines present in the McDonald spectra cannot therefore be ascribed directly to the resolution of those data, again as was concluded during McDonald data analysis (Bleach et al. 2000).

The origin of the inconsistency between the McDonald data Na I doublet and INM lines appears to lie with the EG UMa Na I doublet profile in these data (given the good relationship between the echelle Na I and INM measurements and their reasonable consistency with the McDonald INM data). So what can cause a change in the Na I doublet profile? Well, the profile can be altered as a result of varying the Na I abundance, or by altering the temperature or surface gravity conditions of the star. Although we would not expect to see a global change in these factors on a time-scale such as that between the McDonald and echelle observations, surface inhomogeneities could result in short-term variations and therefore alteration of the line profile. This cannot be ruled out as the origin of the profile variation; however, we consider a more plausible origin lies with inaccurate removal of telluric absorption in the region of the Na I doublet.

Removal of telluric features in the McDonald data was believed to have been achieved successfully; the origin of this confidence was due to the fact that it was possible to observe, at least in good S/N EG UMa spectra, the removal of the more easily identified telluric lines. However, small-scale remnant features may have remained. When the echelle spectra of EG UMa were degraded to the resolution of the McDonald data, it became apparent that these

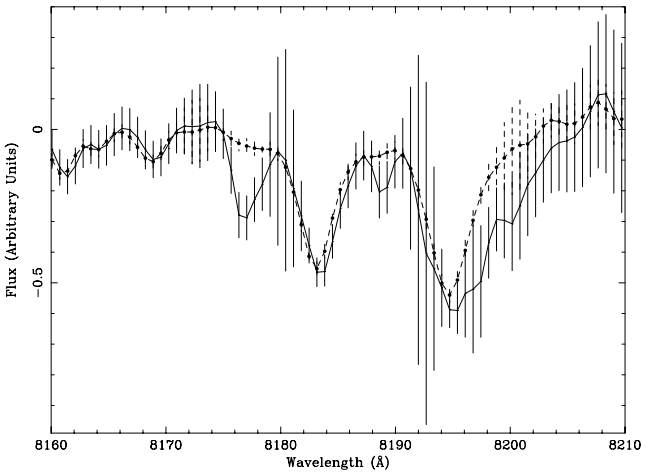

Figure 12. EG UMa Na I doublet in observation 1E degraded to the resolution of the McDonald spectra (broken line) and after the inadequate removal of added telluric absorption (solid line).

observations contained less atmospheric water (see Fig. 11). If water was added, by multiplication with a water template spectrum, then the level of telluric absorption could be enhanced to resemble that in the McDonald spectra. If the subsequent removal of the telluric absorption is not complete, then the remnant Na I doublet can appear broader (see Fig. 12). To test the effect on $V_{\rm rot} \sin i$ of the apparent Na I doublet broadening, observation 1E had water added and subsequently, inadequately, removed and its $V_{\rm rot} \sin i$ value was measured. The Na I $V_{\rm rot} \sin i$ value obtained using Gl 402 was $44 \pm 24\,{\rm km\,s^{-1}}$, which is in agreement with that measured previously (see Table 5), although it is difficult to draw any particular conclusions with such a large error bar. If enough of the McDonald EG UMa spectra have augmented Na I doublet linestrength as a result of unsatisfactory water correction, then it might be possible for this to explain the inaccurate, and overestimated, measurement of $V_{\rm rot} \sin i$. This is particularly true if water correction was applied more successfully in the M star template spectra due to their superior S/N. The McDonald data PG 1026 + 002 Na I doublet also results in a $V_{\rm rot} \sin i$ measurement that exceeds the maximum expected value. Again this could possibly be due to inaccurate telluric absorption removal.

4 HZ 9 AND RE J1629 + 780

4.1 Rotational broadening

We obtained rotation rate, $V_{\rm rot} \sin i$, measurements for HZ 9 and RE J1629 + 780 employing the same technique as for EG UMa (see Section 3.2). Measurements were obtained from the Na I doublet at 8183, 8195 Å and the INM lines (fitting range 8374–8400 and 8410–8430 Å). K I 7698.9 Å line measurements were not obtained, as any investigation was hampered by the limiting position of telluric absorption and/or poor S/N of the single spectra.

4.1.1 HZ 9

To calculate the radial velocity smearing that needed to be applied to the template stars, we fitted a radial velocity curve to the data from Stauffer (1987). The $V_{\rm rot} \sin i$ values obtained from the Na I doublet and INM lines are displayed in Table 6. There is a hint that the Na I $V_{\rm rot} \sin i$ values are higher than those from the INM, but the measurements are in agreement, albeit due to the considerable error bars. Once again we have to acknowledge that the water removal is not completely accurate and could therefore be the origin of any Na I doublet $V_{\rm rot} \sin i$ overestimation. The INM line $V_{\rm rot} \sin i$ is comparable to that measured in EG UMa, which is expected, as these systems have a similar orbital period and secondary star spectral class.

Table 6. Summary of Na I doublet and INM line $V_{\rm rot} \sin i$ measurements obtained from the PCEBs HZ 9 and RE J1629 + 780. The template M stars Gl 402 and GL 447 were employed.

Object	Template	$V_{\rm rot} \sin i$ (km s^{-1}) Na I doublet	INM
HZ 9	Gl 402	38.5 ± 10.0	32.0 ± 6.5
HZ 9	Gl 447	40.0 ± 8.5	31.0 ± 7.0
RE J1629+780	Gl 402	28.5 ± 5.0	24.0 ± 4.5
RE J1629+780	Gl 447	26.5 ± 5.0	23.0 ± 4.0

4.1.2 RE J1629 + 780

No smearing was incorporated into the measurements for RE J1629 + 780, as the secondary star lacks any significant radial velocity variation (Section 1.3). The $V_{\rm rot} \sin i$ values obtained from the Na I doublet and INM lines are displayed in Table 6. The measurements from the Na I doublet and INM lines are in agreement, and suggest a projected rotational velocity similar to that exhibited by the secondary stars in EG UMa and HZ 9. As discussed in Section 1.3, the lack of observed secondary star radial velocity variation led to the suggestion of two possible system configurations; the component stars of the binary are widely separated or RE J1629 + 780 is a very low-inclination system. The measurement of $V_{\rm rot} \sin i$ implies that we are not observing RE J1629 + 780 pole-on, and therefore suggests that this is a wide binary system.

5 CONCLUSIONS

We measure the projected rotational velocity, $V_{\rm rot} \sin i$, of the secondary star in EG UMa from the Na I doublet at 8183, 8195 Å ($31.2 \pm 3.7\,{\rm km\,s^{-1}}$), from the Fe and Ti intrinsically narrow metal (INM) lines in the region 8374–8430 Å (26.6 ± 2.7 and $27.8 \pm 3.0\,{\rm km\,s^{-1}}$) and the K I line at 7698.9 Å ($26.2 \pm 3.5\,{\rm km\,s^{-1}}$). The disagreement between $V_{\rm rot} \sin i$ values measured from the 8183, 8195 Å Na I doublet and the nearby INM lines, as displayed in previous medium-resolution data (Bleach et al. 2000; Catalán et al. 2002a; Catalán et al. 2002b), is not present in the PCEB high-resolution data. In addition, the value of $V_{\rm rot} \sin i$ measured for the secondary star in EG UMa from the K I 7698.9 Å line is in agreement with the Na I and INM measurements. There is therefore a reassuring consistency in the value of $V_{\rm rot} \sin i$ measured from different secondary star photospheric lines. The values of $V_{\rm rot} \sin i$ measured from the high-resolution EG UMa spectra are also consistent with that expected from system parameters derived from previous observational data.

Obtaining a suitable template star for $V_{\rm rot} \sin i$ measurement seems relatively straightforward. This is due to the value of $V_{\rm rot} \sin i$ measured lacking a strong dependence on the template star employed. The INM line $V_{\rm rot} \sin i$ measurements show a particularly good level of consistency, apparently being devoid of any spectral type dependence, at least in the spectral range M0/1V to M4/5V.

The INM lines could therefore be extremely useful for measuring the rotational broadening of the secondary stars in CV and LMXB systems where the spectral typing of the secondary star can be problematic.

We measure a $V_{\rm rot} \sin i$ value of 34.3 ± 3.8 km s^{-1} for the secondary star in HZ 9. This value, measured from the Na I doublet and the INM lines, is similar to the value measured for EG UMa. This is expected, as these systems share a similar orbital period and secondary star spectral type.

The $V_{\rm rot} \sin i$ of the secondary star in RE J1629 + 780 was measured, again from the Na I doublet and the INM lines, to be 25.1 ± 2.3 km s^{-1}. The measurement of $V_{\rm rot} \sin i$ in RE J1629 + 780 indicates that this system, which lacks radial velocity shifts due to orbital motion, is a wide binary as opposed to a low-inclination system.

ACKNOWLEDGMENTS

We thank Tom Marsh for the use of his MOLLY routine. The William Herschel Telescope is operated on the Island of La Palma by the ING at the Observatorio del Roque de los Muchachos of the Instituto Astrofisica de Canarias. JNB is supported by a Royal Society–JSPS Fellowship.

REFERENCES

Allard F., Hauschildt P. H., 1995, ApJ, 445, 433
Bleach J. N., 2001, PhD thesis, Keele Univ.
Bleach J. N., Wood J. H., Catalán M. S., Welsh W. F., Robinson E. L., Skidmore W., 2000, MNRAS, 312, 70 (McDonald data)
Casares J., Charles P. A., 1994, MNRAS, 271, L5
Catalán M. S., Sarna M. J., Jomaron C. M., Smith R. C., 1995, MNRAS, 275, 153
Catalán M. S., Smith R. C., Jones D. H. P., 2002a, submitted
Catalán M. S., Welsh W. F., Wood J. H., 2002b, submitted
Cooke B. A. et al., 1992, Nat, 355, 61
Delfosse X., Forveille T., Perrier C., Mayor M., 1998, A&A, 331, 581
Eggen O. J., Greinstein J. L., 1965, ApJ, 141, 83
Gliese W., Jahreiss H., 1991, Third Catalogue of Nearby Stars, preliminary version, available at CDS Strasbourg
Gray D. F., 1992, The Observation and Analysis of Stellar Photospheres. Cambridge Univ. Press, Cambridge
Greenstein J., 1958, Handbuch der Physik, 50, 161
Greenstein J. L., 1965, in Luyten W. J., ed., First Conf. on Faint Blue Stars. Univ. Minnesota Press, Minneapolis, p. 97
Guinan E. F., Sion E. M., 1984, AJ, 89, 1252
Hauschildt P. H., Baron E., Allard F., 1997, ApJ, 483, 390
Horne K., Welsh W. F., Wade R. A., 1993, ApJ, 410, 357
Humason M. L., Zwicky F., 1947, ApJ, 105, 85
Iben I., Livio M., 1993, PASP, 105, 1373
Iben I., Tutukov A. V., 1993, ApJ, 418, 343
Lanning H. H., 1982, ApJ, 253, 752
Lanning H. H., Pesch P., 1981, ApJ, 244, 280
Marsh T. R., Robinson E. L., Wood J. H., 1994, MNRAS, 266, 137
Mills D., Webb J., Clayton M., 1997, Starlink User Note 152.4
Nicholls R., 1988, J. Quant. Spectrosc. Radiat. Transfer, 40, 275
Paczyński B., 1976, in Eggleton P. P., Mitton S., Whelan J., eds, Proc. IAU Symp. 73, Structure and Evolution of Close Binary Systems. Reidel, Dordrecht, p. 75
Pesch P., 1968, ApJ, 151, 605
Pounds K. A. et al., 1993, MNRAS, 260, 77
Probst R. G., 1984, ApJ, 53, 335
Reid I. N., Hawley S. L., Gizis J. E., 1995, AJ, 110, 1838
Rothman L. S. et al., 1998, J. Quant. Spectrosc. Radiat. Transfer, 60, 665
Sandquist E. L., Taam R. E., Chen X., Bodenheimer P., Burkert A., 1998, ApJ, 500, 909
Schiavon R. P., Barbuy B., Rossi S. C. F., Milone A., 1997, ApJ, 479, 902
Shahbaz T., Wood J. H., 1996, MNRAS, 282, 362
Shortridge K. et al., 1999, Starlink User Note 86.17
Sion E. M., Wesemael F., Guinan E. F., 1984, ApJ, 279, 758
Sion E. M., Holberg J. B., Barstow M. A., Kidder K. M., 1995, PASP, 107, 232
Smith R. C., Sarna M. J., Catalán M. S., Jones D. H. P., 1997, MNRAS, 287, 271
Stauffer J. R., 1987, AJ, 94, 996
Stephenson C. B., 1960, PASP, 72, 387
Wade R. A., Horne K., 1988, ApJ, 324, 411

This paper has been typeset from a TEX/LATEX file prepared by the author.